DAWN-VIR AT VESTA AND CERES: WRAP-UP OF THE CORRECTIONS FOR THE DATA OF THE VISIBILE CHANNEL.

B. Rousseau[1], M. C. De Sanctis[1], A. Raponi[1], M. Ciarniello[1], E. Ammannito[2], A. Frigeri[1], F. G. Carrozzo[1], P. Scarica[1], S. Fonte[1], F. Tosi[1]. [1]IAPS-INAF, Via Fosso del Cavaliere, 100, 00133 Rome, Italy (batiste.rousseau@inaf.it), [2]ASI, Via del Politecnico, 00133, Rome Italy.

Introduction: The Visible and InfraRed mapping spectrometer (VIR) was carried onboard the NASA Dawn mission [1] to study the spectral properties of the surface of the large asteroid Vesta and the dwarf planet Ceres in the visible to near infrared range.

VIR is a mapping spectrometer made of two independent channels, the first operating in the visible (VIR-VIS, 0.25-1.07µm) and the second in the infrared (1.02-5.09µm). Here we focus on the visible data set. Examples are given for Ceres but are valid also for Vesta data.

It has been observed that the data produced by VIR-VIS suffered of instrumental effects related to the temperature of the detectors: 1) spectral reddening with the increasing temperature of the visible detector (a charge coupled device - CCD); 2) spectral distortion when the temperature of the infrared detector is high [2].

Here we report two corrections which have been implemented to improve the VIR-VIS data [2,3,4]: we first explain how a refinement of the correction dedicated to the global spectral shape – independent of the detectors' temperatures – of the VIR-VIS spectra has been derived. Then, we detail the correction of the spectral dependence to the detectors' temperatures, which improved the analysis of the VIR-VIS data.

Refinement of the Spectral Correction: VIR data have been previously corrected, using ground-based observations, to remove a spurious positive slope affecting the spectra [5]. Recently, this correction has been refined [3] through a five-steps approach: 1) Ceres ground observations are collected on the basis of their consistency, considering the range where they overlap [6-13]; 2) those full-disk observations are converted in bidirectional reflectance at standard geometry (incidence angle = 30°, emergence angle = 0°, phase angle = 0°), using the Hapke theory [14] and the photometric parameters previously derived for Ceres [15]; 3) a smooth average spectrum is computed using the spectra obtained in (2); 4) VIR data are converted at the same standard geometry and an average spectrum is calculated; 5) the last step consists in the calculation of the ratio between the spectrum derived from the ground-based observations (3) and the VIR average spectrum (4). The obtained ratio is a multiplicative factor that is used to correct every spectrum of VIR-VIS, acquired at Ceres but also at Vesta.

Spectral Dependency to the CCD Temperature: VIR data are acquired in sequences of several hyperspectral cubes (typically 6 at a time). During a sequence, the CCD is used for several hours and its temperature increase all along, before to cooling down passively when it is not operating, i.e. in between two sequences. This is illustrated by Fig. 1 which displays a map of the hyperspectral cubes acquired during the Ceres Science HAMO (CSH) mission phase. The color scale shows the CCD temperature, the darker the colder. The black arrow shows a sequence within which the CCD temperature starts at 169K and ends at 184K after 2.5 h of operation.

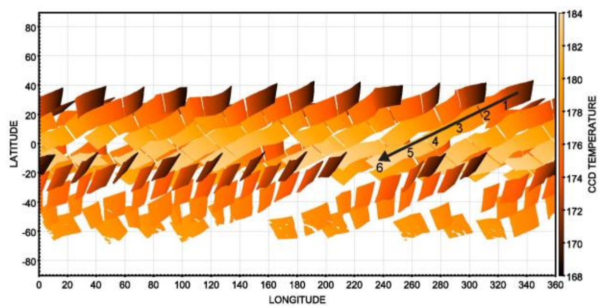

Figure 1 - Map of the VIR-VIS cubes acquired during the CSH mission phase at Ceres. The detector temperature increases during a sequence, made of several cube (black arrow).

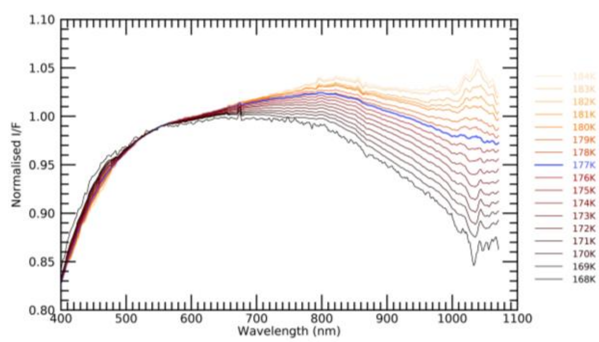

Figure 2 - Median spectra of the Ceres Science HAMO mission phase normalized at 550nm. Each spectrum corresponds to a CCD temperature bin. The blue spectrum is the reference one (see text).

The results of the CCD temperature increase is revealed in Fig. 2 where a median spectrum is calculated for each bin of CCD temperature for the CSH mission phase. A distinct reddening is observed with the rising CCD temperature. To overcome this issue, we adopted a strategy allowing to correct both Vesta and Ceres data set, while considering the special cases that have been encountered.

Correction: During the cruise phase of the Dawn spacecraft, VIR observed the star Arcturus. Since this observation matches with ground-based observations done at a similar spectral resolution [16-18], we consider the temperature of the detectors recorded at this time to build a spectral reference. Thus, the latter is calculated as an averaged spectrum of acquisitions made at 177K (CCD temperature) and 80K (infrared detector (IR) temperature), with data collected in a mission phase which provided an important and representative spatial coverage (CSH for Ceres, Vesta Science HAMO 2 (VH2) for Vesta). We then defined a correction factor defined as follow:

$$CF_{X,\lambda,T} = \left({}^{I}/_{F}\right)_{X,\lambda,T} / \left({}^{I}/_{F}\right)_{X_{ref},\lambda,177K}$$

where I/F refers to the calibrated radiance factor normalized at 550 nm, X to the mission phase name to be corrected, X_{ref} is the reference mission phase (VH2 or CSH), λ is the wavelength and T the CCD temperature.

The correction factors are consequently calculated for each bin of temperature and for a given mission phase. In practice, this is applied as a wavelength-dependent correction, individually on each spectrum, by interpolating the CCD temperature recorded at the time of the observation.

Because the various mission phases may have experience different CCD temperature ranges, or may have a high IR temperature and/or other particularities (e.g. changing exposure time), a single correction factor is not enough and several one must be calculated ([2, 4] for more details).

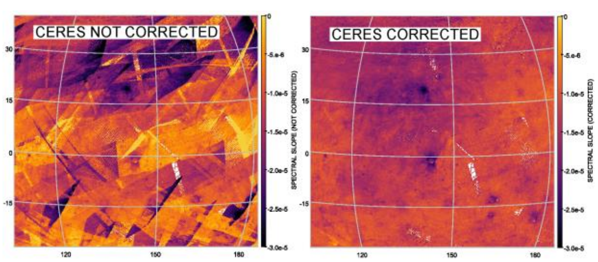

Figure 3 - Map of the spectral slope in the interval 630-950 nm for the Ceres' Dantu region before (left) and after (right) the correction for the CCD temperature dependency.

Results: To highlight the outcome of this empirical correction, we use the spectral slope in the interval 630-950nm (for Ceres) as an example. Fig. 3 gives an illustration of the efficiency of the correction by showing a map of the Dantu region before and after applying the correction. Details and features on the surfaces become visible on this map, made up of several hyperspectral cubes.

Conclusion: In addition to an improvement of the calibration, an empirical correction has been developed to overcome the spectral issues linked to the detectors' temperature affecting the data acquired by VIR in the visible range. This correction now enables the study (mapping, spectral analysis, modelling, etc.) of the rich data set acquired by VIR-VIS at Ceres [3] and Vesta [19] (see also Rousseau et al., this conference).

The corrections reported here have been developed and adapted for the data set of Ceres [2] and Vesta [4]. The calibration refinement is also reported in [3].

The corrected data will be delivered to the Planetary Data System archive (https://pds-smallbodies.astro.umd.edu/data_sb/missions/dawn/index.shtml).

Acknowledgments: VIR is funded by the Italian Space Agency (ASI) and was developed under the leadership of INAF-Istituto di Astrofisica e Planetologia Spaziali, Rome, Italy (Grant ASI INAF I/004/12/0). The instrument was built by Selex-Galileo, Florence, Italy. The authors acknowledge the support of the Dawn Science, Instrument, and Operations Teams.

References: [1] De Sanctis M. C. et al. (2011) *Space Sci. Rev.*, 163, 329. [2] Rousseau B. et al. (2019) *Rev. Sci. Instrum.*, 90, 123110. [3] Rousseau B. et al. (2020) *A&A*, 642, A74. [4] Rousseau B. et al. (2020) *Rev. Sci. Instrum*., 91, 123102. [5] Carrozzo F. G. et al. (2016) *Rev. Sci. Instrum*., 87, 124501. [6] Chapman C. R. & Gaffey M. J. (1979) *Asteroids*, 655. [7] Roettger E. & Buratti B. (1994) *Icarus*, 112, 496. [8] Parker, J. W. et al. (2002) *AJ*, 123, 549. [9] Bus S. J. & Binzel R. P. (2002a) *Icarus*, 158, 146. [10] Bus S. J. & Binzel R. P. (2002b) *Icarus*, 158, 106. [11] Lazzaro D. et al. (2006) *ACM IAU Symp*., 229. [12] Li J.-Y. et al. (2006) *Icarus*, 182, 143. [13] Rivkin A. S. et al. (2011) *Space Sci. Rev*., 163, 95. [14] Hapke B. (2012) *Theory of reflectance and emittance spectroscopy*. Cambridge university press. [15] Ciarniello M. et al. (2017) *A&A* 598, A130. [16] Kiehling R. (1987) *A&A Suppl. Ser*., 69, 465. [17] Alekseeva G. A. et al. (1996) *Baltic Astron.*, 5, 603. [18] Rayner J. T. et al. (2009) *Astrophys. J. Suppl. Ser*., 185, 289. [19] Rousseau B. et al, *in prep.*